Twelfth Australasian Fluid Mechanics Conference
The University of Sydney, Australia 1995

MEASUREMENT OF TIME MEAN AND TURBULENCE PARAMETERS OF TURBULENT SWIRLING FLOWS IN AXISYMMETRIC ANNULI

Wei Yang
Department of Chemical Engineering
The University of Melbourne
Parkville, Victoria
Australia

Yos S. Morsi, and Johannes P. van der Walt
Modelling and Diagnostics Group
School of Mechanical & Manufacturing Engineering
Swinburne University of Technology
Hawthorn, Victoria
Australia

ABSTRACT

With the aid of Laser Doppler Anemometry (LDA) and Hot-wire anemometry techniques, turbulent swirling flows inside axisymmetric annuli formed between two concentric stationary cylinders have been examined. The radial variations of the instantaneous axial and tangential velocity components and the wall static pressures at various axial locations along the annulus were determined for Reynolds numbers in a range of 75,000 to 150,000 and inlet swirling angles of 30°, 45° and 60° respectively.

Selected experimental data using LDA technique are presented and discussed. Furthermore, the results are compared with the measurements obtained by the hot-wire technique. Good agreement between Hot-wire and LDA data was found in the core region of the flow. However, near the wall there is a discrepancy between the two sets of data.

INTRODUCTION

Although the presence of swirl is associated with high pressure drops it can introduce some favourable effects to the flow. In combustion systems, such as gasoline engines, gas turbines, industrial furnaces and utility boilers, applying the swirling flows can be very beneficial to the stabilisation of the flame and increases in combustion efficiency. In the case of heat exchangers on the other hand, the introduction of swirling flow increases the rate of heat transfer without paying the penalty of excessive eddy losses associated with wakes shed by tubes and fins. This, in addition to a wide range of applications (including for example cyclone separators, Ranque-Hilsch tubes, diffusers, turbines and jet pumps), necessitates the understanding of such a complex flow which in return requires accurate knowledge of the magnitude and direction of the velocity vectors.

Swirling annular flows are quite complex in nature primarily due to the effect of the curvature which modifies the turbulence structure on the convex and concave walls. Very little work has been published on the turbulent structure of a swirling flow along an annulus. Lacking of data is particularly evident on turbulence intensities, shear stresses and Kinetic energy. However, there are a number of experimental investigations reported in the literature where the time mean axial and tangential velocity distributions were measured (Scott and Rask, 1973; Scott and Bartelt, 1976; Simmers and Coney, 1979), and recently Clayton and Morsi (1984), Clayton and Morsi (1985), Yowakim and Kind (1988) and Solnordal and Gray (1994) performed comprehensive experimental studies on both time mean and turbulent structures of swirling flow inside annuli.

Hot-wire anemometry is the most common measuring technique used by previous workers. However, due to the aerodynamic interference and variations of the flow physical parameters such as temperature, density and pressure, there is always doubt over the accuracy of the experimental data obtained, particularly turbulence parameters.

In this paper, the non-intrusive optical method namely Laser Doppler Anemometry (LDA) is used together with Hot-wire technique to examine the fluid flow structure of turbulent swirling flows inside an annulus.

EXPERIMENTAL RIG

The experimental rig used in this work was initially designed by Solnordal (1992). However, the special design of the traversing mechanism and other modifications necessary to achieve the objectives of the present investigation were developed by Yang (1995). Here only a brief account of the experimental rig is given, however, for a full description of the rig see Solnordal (1992). As shown in Figure 1, the apparatus consists of an annular test section formed of two concentric cylinders with a diameter ratio d_i/d_o = 0.41 and an annular gap of 24.7 mm. The length of the annulus is approximately 3 meters long, 65 hydraulic diameters (x/D_h = 65.0) which ensured a complete decay of the swirl to occur under all operating conditions of the flow. At the inlet a row of 20 guide vanes equispaced around a bellmouth was used to impart free vortex to the air flow along the annulus. The experimental data reported in this paper covers average Reynolds numbers in the range of 75,000 and 150,000, and swirling angles of 30°, 45° and 60° respectively.

LDA FACILITY

In the LDA system, the Dantec two-component fibre optic probe was used. This system consists of a two colour four beam optical arrangement utilising the green (wave length = 514.5 nm) and the blue (wave length = 488 nm) lines of a 5 watt Argon-Ion laser. In order to obtain meaningful data across the annular gap of 24.7 mm, the measurement volume needed to be as small as possible. Therefore, a fibre optic probe lens with a focal length of 100 mm was used to obtain a measurement volume with approximate diameter of 0.05 mm and length of 0.26 mm.

For the seeding of LDA, glycol smoke particles of 0.5 μ m diameter were injected into the annular gap by a smoke generator. The low density particles showed to track the gas flow well within the limit of accuracy of the measurement, including high swirling flows. Their high refractive index was useful in maximising the signal-to-noise ratio (SNR), which assisted in obtaining the maximum data rate and hence more accurate information.

The data were processed using the residence time weighting technique (Buchhave et al., 1979). All the velocities were weighted by the residence times Δt_i of the individual scattering particles. Thus the mean and rms values are given by

$$U = \frac{\sum_{i=1}^{N} U_i \Delta t_i}{\sum_{i=1}^{N} \Delta t_i}$$

and

$$\sqrt{\overline{u^2}} = \left[\frac{\sum_{i=1}^{N} \left(U_i - U\right)^2 \Delta t_i}{\sum_{i=1}^{N} \Delta t_i} \right]^{1/2}$$

in which U is the time mean axial velocity, $\sqrt{\overline{u^2}}$ is the rms value of the axial velocity component, the subscript i denotes the *ith* particle, N is the number of particles so-called sample size, and Δt_i is the transit time of *ith* particle for residence time weighting.

HOT-WIRE ANEMOMETRY FACILITY

A single hot-wire probe rotating technique as described by Tuckey et al (1984) was employed to determine the radial profiles of time mean velocity components and turbulence intensities at various axial locations along the annulus. A special designed traversing mechanism to facilitate the traverse of the probe within 0.1 mm distance across the annular gap was employed in the measurements. The TSI Model IFA 100 Intelligent Flow Analyzer which consists of a constant temperature anemometer, a signal conditioner and one temperature module was used to process output signals from the hot-wire probe. A TSI model 1260-T1.5 hot-wire probe proved to be adequate for the measurement of time mean velocity components and turbulence parameters. The data was recorded and analysed with the aid of an acquisition system known as DASYLab.

RESULTS AND DISCUSSION

The time mean axial and tangential velocity profiles for a Reynolds number of 78,000 and inlet swirl angle of 45° obtained from LDA and Hot-wire are presented for different axial locations along the annulus in Figure 2. The velocities and radial distances are normalised by the average axial velocity at each test station and the annular gap respectively. Successive velocity profiles have been shifted vertically by 0.4 units, so that the axial location of each profile can be distinguished.

As shown in these Figures, the agreement of two sets of data is quite reasonable for the core region of the annular gap particularly as the flow approach the fully developed region (x/D_h>15.8). However, there is a significant discrepancy between the data obtained from LDA and Hot-wire measurements. Such a difference is attributed, in LDA, to optical noise and low data rate (less seeding particles near wall regions) and in hot-wire technique to the possible aerodynamic interference from the prongs of the hot-wire probe and possible heat transfer effect which may reduces the temperature of the wire due to a relatively cold wall. No firm conclusion can be given on which method gives better accuracy of results.

Figure 3 shows the mean tangential velocity distributions again at different axial positions along the annulus. The profiles indicate that the tangential velocity distributions change their characteristics from a free vortex nature at the inlet to a forced vortex at downstream regions of the test section (around $x/D_h \geq 28.0$).

Based on the measured outer wall static pressure, the static pressure distributions across the annular gap were calculated from the numerical integrated equation as follows,

$$P(r) = P_w - \int_r^{r_o} \frac{\rho W^2}{r} dr$$

in which P_w is the measured outer wall static pressure and W is the time mean tangential velocity.

The normalised (by the average axial dynamic pressure) static pressure distributions along the annulus for Reynolds number of 78,000 and 75,000 and inlet swirl angles of 45° and 60° are shown in Figure 4. As expected, all pressure gradients show an increasing variation from inner wall to outer wall. Furthermore the pressure difference between the inner and the outer walls decreases as the swirl decays along the annulus. In the case of a high inlet swirl angle, the increased value of the static pressure across the gap is approximately 87% of the outer wall static pressure at the first test station at x/D_h = 5.4, comparing to only 4.6% increased of pressure at x/D_h = 65.

The axial and tangential components of turbulence intensities are presented in terms of Reynolds normal stress, of ρu^2 and ρw^2 ; where u^2 and w^2 are the squared values of measured rms components in the axial and tangential directions respectively.

The normalised axial and tangential components of Reynolds normal stress for Reynolds number of 150,000 and inlet swirl angle of 45° are presented in Figure 5. As expected, due to the large velocity gradients, the high stress regions of both axial and tangential components are found in the vicinity of the inner and outer walls.

The results also show that even for a swirl angle of 45°, the axial normal stress, in the upstream locations of $x/D_h <$ 15.8, is almost twice as much as the tangential normal stress. As the flow decays along the annulus the flow becomes almost isotropic hence the axial and tangential normal stresses are approximately equal.

CONCLUSIONS

The following conclusions can be drawn from the present experimental investigation:

(1) The agreement between the results obtained using the two measuring techniques is good in the core region only. Near the walls however, there is some difference between the data obtained from LDA and Hot-wire methods.

(2) As the inlet swirl intensity increases, the rate of the decay of the swirl increases.

(3) The maximum of the tangential velocity component shifts form the inner to the outer walls as the flow progresses downstream.

(4) All pressure gradients are higher near the inner wall than the outer wall. The pressure difference between two walls decreases as flow develops along the annulus.

(5) For the range of swirl intensity investigated here the axial normal stress are higher than radial and tangential in the developing region of the flow. As the swirl decays and develops along the annulus the difference between the values of axial, radial and tangential stress decreases.

(6) Isotropic turbulence can not be assumed in the developing region of the flow, in the fully developed region however, the assumption of isotropic turbulence may be hold.

REFERENCES

Buchhave, P., George, W. K. and Lumley, J. L., 1979, "The Measurement of Turbulence with the Laser-Doppler Anemometer", *Annual Review of Fluid Mechanics*, Vol. 11, pp.443-503

Clayton, B.R. and Morsi, Y.S.M., 1984, "Determination of Principal Characteristics of Turbulent Swirling Flow along Annuli, Part 1: Measurement of Time Mean Parameters", *International Journal of Heat Fluid Flow*, Vol. 5, No. 4, pp.195-203.

Clayton, B.R. and Morsi, Y.S.M., 1985, "Determination of Principal Characteristics of Turbulent Swirling Flow along Annuli, Part 2: Measurement of Turbulence Components", *International Journal of Heat Fluid Flow*, Vol. 6, No. 1, pp.31-41.

Scott, C. J. and Rask, D. R., 1973, "Turbulent Viscosities for Swirling Flow in a Stationary Annulus", *Journal of Fluids Engineering, Transaction of ASME*, Vol. 95, pp.557-566.

Scott, C. J. and Bartelt, K. W., 1976, "Decaying Annular Swirl Flow with Inlet Solid Body Rotation", *Journal of Fluids Engineering, Transaction of ASME*, Vol. 98, pp.33-40.

Simmers, D. A. and Coney, J. E. R., 1979, "The Experimental Determination of Velocity Distribution in Annular Flow", *International Journal of Heat and Fluid Flow*, Vol. 1, No. 4, pp.177-184.

Solnordal, C. B., 1992, "Modelling of Fluid Flow and Heat Transfer in Decaying Swirl Through a Heated Annulus", Ph.D. Thesis, The University of Melbourne.

Solnordal, C. B. and Gray, N. B., 1994, "An Experimental Study of Fluid Flow and Heat Transfer in Decaying Swirl through a Heated Annulus", *Experiments in Fluids*, Vol. 18, pp.17-25.

Tuckey, P. R., Morsi, Y. S. and Clayton, B. R., 198, "The experimental Analysis of Three Dimensional Flowfields", *International Journal of Mechanical Engineering Education*, Vol. 12, No. 3, pp.149-166.

Yang, W., 1995, "Experimental and Numerical Investigations of Turbulent Swirling Flow inside an Annulus", Masters Thesis, Swinburne University of Technology.

Yowakim, F. M. and Kind, R. J., 1988, "Mean Flow and Turbulence Measurements of Annular Swirling Flows", *Journal of Fluids Engineering, Transactions of ASME*, Vol. 110, pp.257-263.

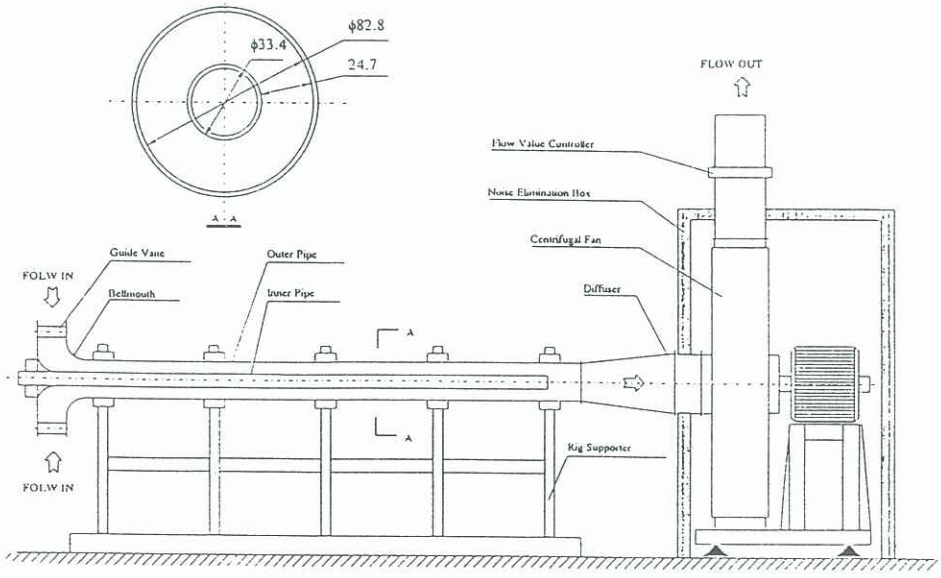

Figure 1 A schematic layout of the experimental rig

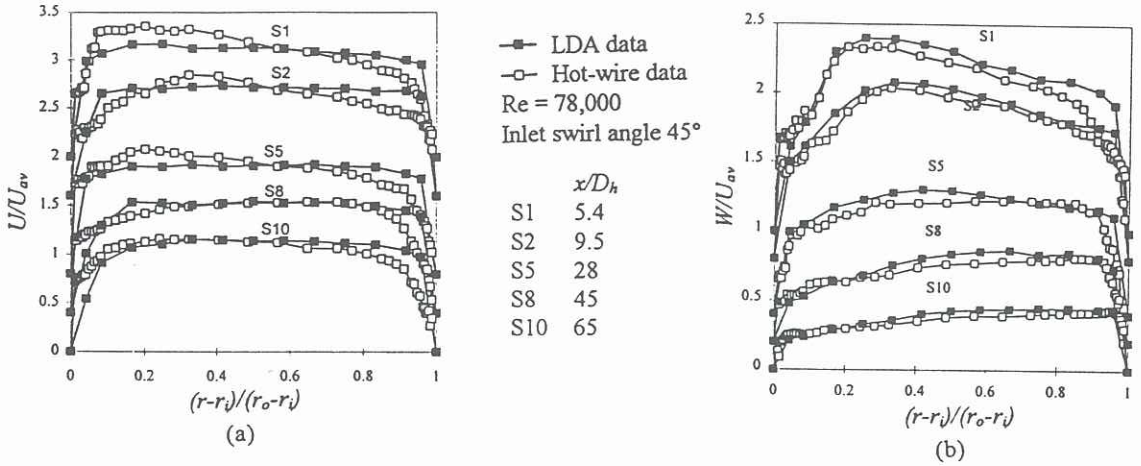

Figure 2 Time mean axial and tangential velocity distributions

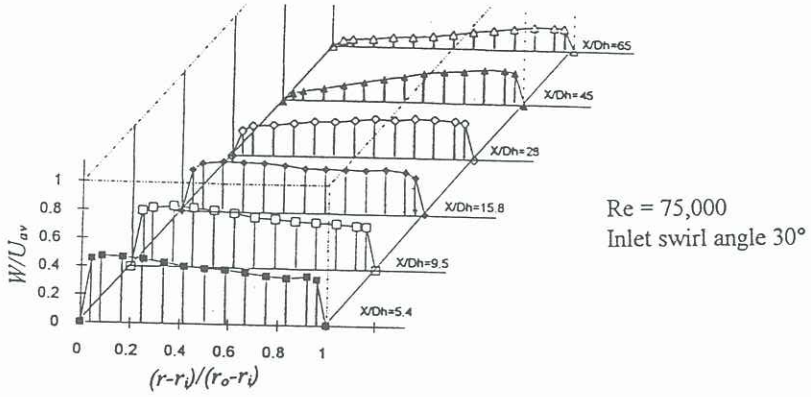

Figure 3 Time mean tangential velocity distributions

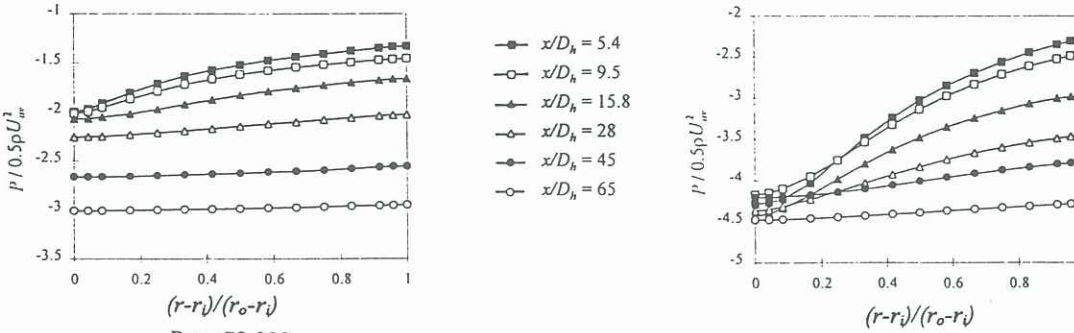

Figure 4 Static pressure distributions

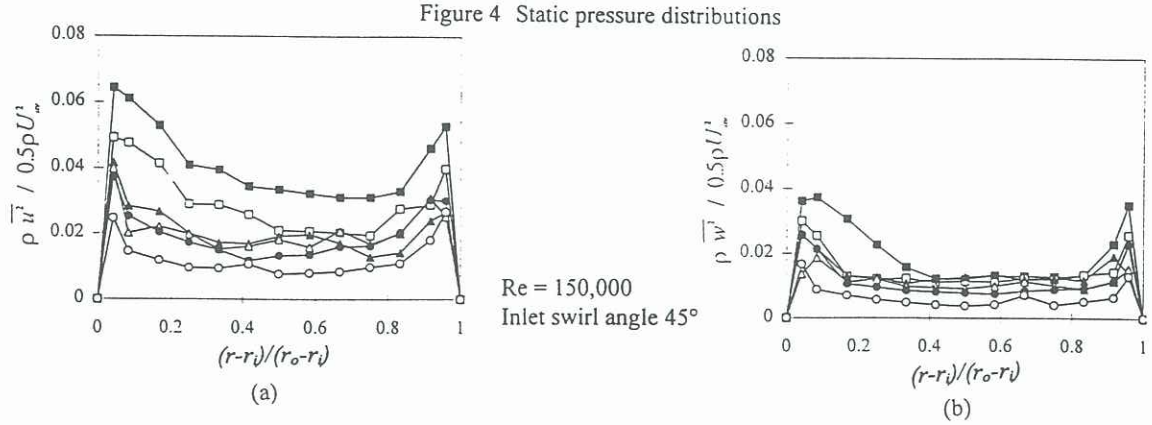

Figure 5 Axial and tangential Reynolds normal stress distributions